International Journal of Innovative Computing, Information and Control
Volume **21**, Number **4**, August **2025**

 ISSN 1349-4198
pp. **937–953**

OPTIMAL SURFACE IN PLAN FOR STRIP FOOTINGS ASSUMING THAT THE CONTACT SURFACE WITH SOIL WORKS PARTIALLY UNDER COMPRESSION

Inocencio Luévanos-Soto[1], Arnulfo Luévanos-Rojas[2,*] and Rosa Margarita Luévanos-Soto[2]

[1]Facultad de Ingeniería, Ciencias y Arquitectura
Universidad Juárez del Estado de Durango, Unidad Gómez Palacio
Av. Universidad S/N, Fracc. Filadelfia, CP 35010, Gómez Palacio, Durango, México
inocencio.luevanos@ujed.mx

[2]Instituto de Investigaciones Multidisciplinaria
Facultad de Contaduría y Administración
Universidad Autónoma de Coahuila, Unidad Torreón
Blvd. Revolución 151 Ote. CP 27000, Torreón, Coahuila, México
r_luevanos@uadec.edu.mx
*Corresponding author: arnulfoluevanos@uadec.edu.mx

Received December 2024; revised March 2025

Abstract. *This paper presents a model to estimate the minimum surface in plan of a strip footing supporting a masonry wall or a concrete wall (uniformly distributed load), assuming that the soil is elastic, the soil pressure distribution is linear and the surface in contact with the soil works partiality in compression. The formulation is developed by integration to estimate the resultant force "R" and a moment about the X axis "M_x". Three cases are shown: Case I) When the area works entirely in compression; Case II) When the area works partially in compression and the neutral axis falls within the flanges; Case III) When the area works partially in compression and the neutral axis falls within the web. Some works assume uniform soil pressure with the wall located at the center of the footing, but do not consider the property boundaries that may occur in some cases. Eight numerical examples are shown for determining the ground contact area for strip footings under a uniformly distributed load. The main savings of the new model compared to the current model are given in w_e (width of the outer footing) $\neq w_i$ (width of the inner footing) with 93.25%, while for $w_e = w_i$ with 98.47%.*

Keywords: Optimal area, Strip footings, Linear soil pressure distribution, Contact surface partially compressed

1. **Introduction.** The strip footing is a type of shallow foundation that is responsible for receiving the entire load of the walls of a construction. Its structure involves a flat horizontal slab placed directly on the ground, to which columns with special characteristics are added that make them the base support for the walls of the building.

There are two types of footings that are best known in the construction world: strip footings and isolated footings. Although both are shallow foundations, they are used for specific purposes. The most important characteristic that makes them different from each other is that strip footings support the weight of an entire wall, while isolated footings only support the weight of a column. On the other hand, in the case of strip footings, the weight is supported in only one direction, while isolated footings have reinforcement in two directions perpendicular to each other.

DOI: 10.24507/ijicic.21.04.937

Some studies show models to estimate the contact area in plan for various types of foundations: Isolated footings (rectangular, square and circular) subjected to biaxial bending [1-10]; Combined footings (rectangular, trapezoidal, strap, T-shaped and L-shaped or corner) subjected to biaxial bending in each column [11-15]; Foundation slabs [16]. These studies assume that the contact surface in plan works entirely in compression.

Several works present models for the complete design of footings for various types of foundations: Isolated footings (rectangular, square and circular) subjected to biaxial bending [17-21]; Combined footings (rectangular, trapezoidal, strap, T-shaped and L-shaped or corner) subjected to biaxial bending in each column [22-29]. These works assume that the contact surface in plan operates entirely in compression.

Other authors propose models to estimate the contact surface in plan for various types of foundations assuming that the contact surface of the soil works partially to compression and the distribution of the soil pressure is linear: Isolated footings (rectangular, square and circular) subjected to biaxial bending [30-42]; Rectangular combined footings subjected to biaxial bending in each column [43].

Some papers show the complete design of footings for various types of foundations assuming that the contact surface of the soil works partially to compression and the distribution of the soil pressure is linear: Isolated footings (rectangular, square and circular) subjected to biaxial bending [44-46].

The studies on strip footings: Saleh et al. investigated the bearing capacity behavior of strip footings subjected to eccentric and inclined loads through laboratory work and numerical analysis [47,48]. Farzaneh et al. [49] studied the seismic bearing capacity for strip footings subjected to concentric loads and the footings are located near cohesive slopes using lower bound limit analysis. Sadoglu [50] developed an optimal model for the design of a strip footing subjected to a horizontal load and a vertical load. Fang and Shi [51] presented the lower limit solution of the load-bearing capacity of the foundation under the strip footing according to Mohr's parabolic failure criterion. Keawsawasvong and Ukritchon [52] developed a practical method for the optimal design of a strip footing subjected to a horizontal load and a vertical load. Mazouz et al. [53] showed a numerical analysis performed to obtain the effect of underground void on the load-bearing capacity of a strip footing located on a geogrid-reinforced and non-geogrid-reinforced sand slope with a void inside. Yalaoui et al. [54] evaluated a strip footing settlement and bearing capacity in sandy soil used geotextile and compared the unreinforced and reinforced soil foundations by numerical analysis. Pusadkar et al. [55] investigated the bearing capacity of strip footings resting on soils with multiple square voids. Jaiswal et al. [56] presented the efficiency of strip footing on sand bed reinforced with multilayer geotextile with wraparound ends.

According to the literature review, there are various works that study the behavior of the load capacities and settlements of strip footings on the ground and for their sizing they use the ratio of the load capacity of the soil, which is equal to the load of the wall divided by the area (area working fully in compression), and other works are presented to determine the minimum area and dimensions of rectangular and circular isolated footings assuming that the surface in contact with the ground works partially in compression. Therefore, there is no paper on the subject of optimal surface in plan for strip footings assuming that the contact surface with soil works partially to compression.

This paper shows a model to find the minimum surface in plan of a strip footing supporting a uniformly distributed load due to masonry or concrete walls, assuming that the soil pressure distribution is linear, the soil is elastic, and the surface in contact with the soil works partiality in compression. The methodology is formulated by integration to determine the resultant force "R" and a moment about the X axis "M_x". Three cases

are developed: Case I) When the area works entirely in compression or current model; Case II) When the area works partially in compression and the neutral axis falls within the flanges; Case III) When the area works partially in compression and the neutral axis falls within the web. Some authors assumed that the area of the footing is equal to the wall load divided by the bearing capacity of the soil because the wall located at the center of the footing, but do not consider the property boundaries that may occur in some cases (This study presented in this paper assumes the property boundary condition). Eight numerical examples are shown for determining the ground contact area for strip footings under a uniformly distributed load to verify.

The paper is structured as follows. Section 2 describes the formulation of the model to determine the dimension of the strip footings assuming that contact surface with the ground works partially to compression. Section 2.1 shows the equations for Case I (Area works entirely in compression). Section 2.2 presents the equations for Case II (Area works partially in compression and the neutral axis falls within the flanges). Section 2.3 shows the equations for Case III (Area works partially in compression and the neutral axis falls within the web). Section 2.4 presents the optimal surface for strip footings of the three cases. Section 3 shows the numerical examples applied of the three cases for strip footings. Section 4 presents the results. Section 5 shows the conclusions to complete the paper.

2. **Formulation of the Model.** Figure 1 shows two types of strip footings under biaxial bending. Figure 1(a) presents a strip footing supporting a masonry wall. Figure 1(b) shows a strip footing supporting a concrete wall.

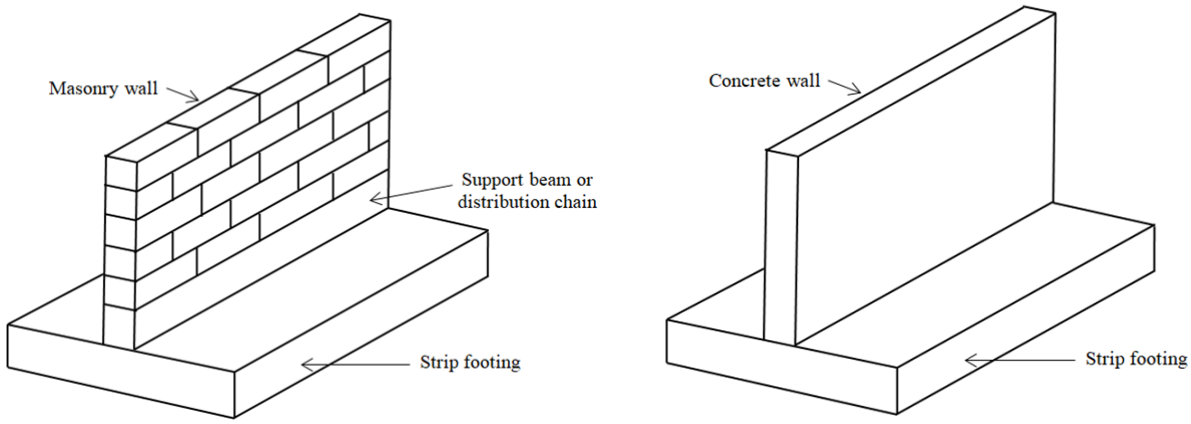

(a) Strip footing supporting a masonry wall (b) Strip footing supporting a concrete wall

FIGURE 1. Strip footing

The pressure generated by the soil "p_s" anywhere on the foundation is

$$p_s = \frac{P}{A} + \frac{M_x y}{I_x} + \frac{M_y x}{I_y} \tag{1}$$

where A = contact surface in plan of the foundation in m^2, P = axial load applied to the foundation in kN, M_x and M_y = moments applied on their respective axes, x and y = coordinates of the foundation under study in kN-m, I_x and I_y = moments of inertia on their respective axes in m^4.

The solution to this type of footings is too simple. Since the first part of Equation (1) is used, that is, only P/A, there is no information when the walls are located on the property boundary.

To solve the problem of walls on the property limits is shown in Figure 2. Figure 2(a) shows a transverse footing to the edge footing. Figure 2(b) presents two transverse footings to the edge footing.

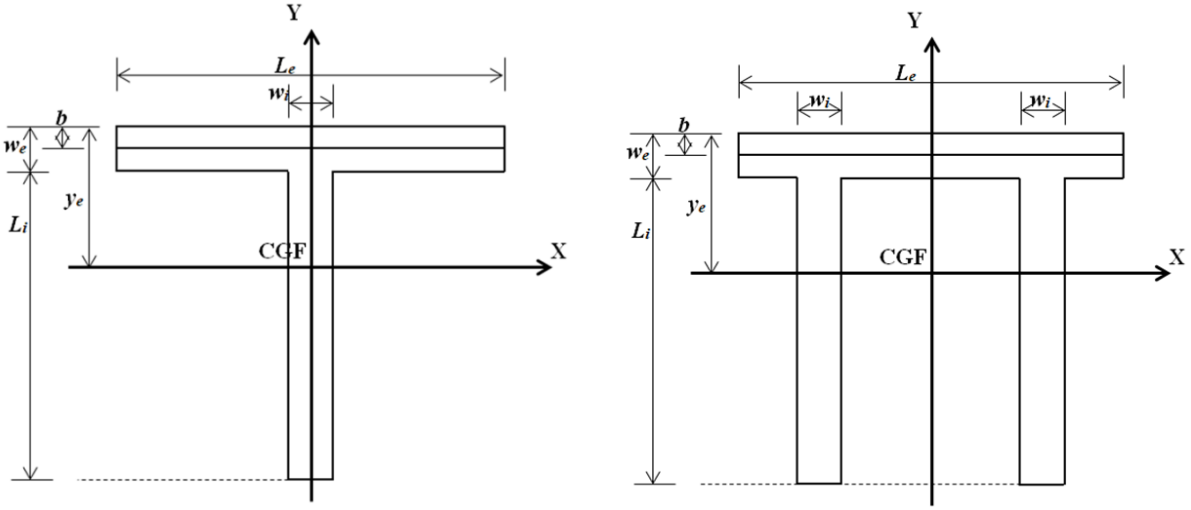

(a) A transverse footing (b) Two transverse footings

FIGURE 2. Strip footing on the property boundary

In addition, "n" transverse footings to the edge footing can be considered.
Properties of the plan section of the footing are

$$A = L_e w_e + nL_i w_i \tag{2}$$

$$y_e = \frac{L_e {w_e}^2 + nL_i w_i (L_i + 2w_e)}{2(L_e w_e + nL_i w_i)} \tag{3}$$

$$I_x = \frac{L_e {w_e}^3 + n w_i {L_i}^3}{12} + L_e w_e \left(\frac{2y_e - w_e}{2}\right)^2 + nL_i w_i \left(\frac{2y_e - L_i - 2w_e}{2}\right)^2 \tag{4}$$

where L_e = exterior wall length in m, L_i = inner wall length in m, w_e = width of the outer footing in m, w_i = width of the inner footing in m, n = number of transverse footings to the edge footing, y_e = distance from center of footing to outer edge in m, I_x = moment of inertia about the X axis.

Note: The moment about the Y axis and the moment of inertia about the Y axis are not considered here, because it is assumed that the section is symmetrical with respect to the Y axis.

In this study, three cases are shown. Case I: When the area works totally in compression or current model. Case II: When the area works partially in compression and the neutral axis falls within the flanges. Case III: When the area works partially in compression and the neutral axis falls within the web.

2.1. **Case I.** When the area works totally in compression or current model (only moment about the X axis, and the moment about the Y axis is zero) as shown in Figure 3.

Substituting $M_y = 0$, A, y_e and I_x into Equation (1), the pressure at each vertex is determined:

$$p_{s1} = p_{s2} = \frac{R}{A} + \frac{M_x y_e}{I_x} \tag{5}$$

$$p_{s3} = p_{s4} = p_{s5} = p_{s6} = \frac{R}{A} + \frac{M_x (y_e - w_e)}{I_x} \tag{6}$$

$$p_{s7} = p_{s8} = \frac{R}{A} + \frac{M_x \left(y_e - L_i - w_e\right)}{I_x} \tag{7}$$

where R is the resultant force produced by the two walls in kN, y_e is the distance from the center of the foundation to the positive extreme fiber in m, w_e is the width of the exterior wall in m, and L_i is the length of the interior wall in m.

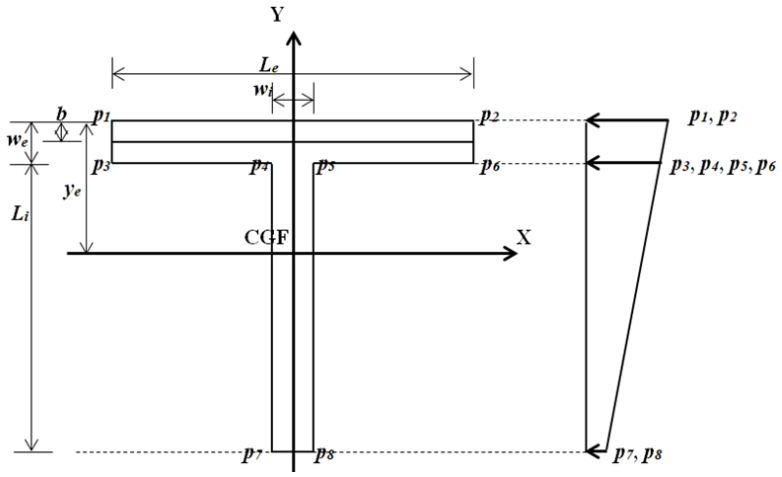

FIGURE 3. Case I or current model

The resultant force is

$$R = P_1 + P_2 \tag{8}$$

where $P_1 = w_1 L_e$ and $P_2 = n w_2 (L_i + w_e - b)$.

The moment about the X axis is

$$M_x = P_1 \left(y_e - \frac{b}{2}\right) + P_2 \left(\frac{L_i + w_e + b}{2} - y_e\right) \tag{9}$$

where w_1 = exterior wall load in kN/m, w_2 = interior wall load in kN/m, b = exterior wall width in m.

2.2. **Case II.** When the area works partially in compression, the neutral axis falls within the flanges $w_y \leq w_e$ (only moment about the X axis, and the moment about the Y axis is zero) as shown in Figure 4.

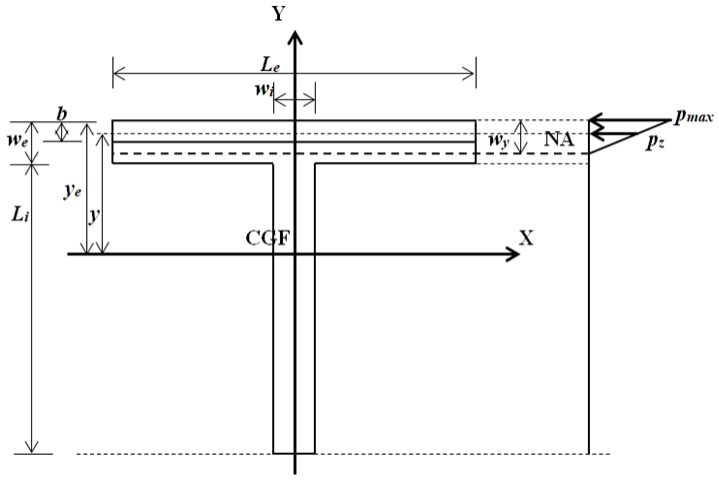

FIGURE 4. Case II

By pressure ratio it is

$$\frac{p_z}{w_y - y_e + y} = \frac{p_{\max}}{w_y} \tag{10}$$

The pressure at anywhere of the footing is determined as follows:

$$p_z = \frac{p_{\max}(w_y - y_e + y)}{w_y} \tag{11}$$

The resultant force is

$$R = -\int_{y_e - w_y}^{y_e} \int_{-\frac{L_e}{2}}^{\frac{L_e}{2}} p_z dx dy \tag{12}$$

Substituting Equation (11) into Equation (12) gives the following:

$$R = -\frac{p_{\max} w_y L_e}{2} \tag{13}$$

The moment about the X axis is

$$M_x = -\int_{y_e - w_y}^{y_e} \int_{-\frac{L_e}{2}}^{\frac{L_e}{2}} p_z y dx dy \tag{14}$$

Substituting Equation (11) into Equation (14) gives the following:

$$M_x = -\frac{p_{\max} w_y L_e (3y_e - w_y)}{6} \tag{15}$$

2.3. **Case III.** When the area works partially in compression, the neutral axis falls within the web $w_y \geq w_e$ (only moment about the X axis, and the moment about the Y axis is zero) as shown in Figure 5.

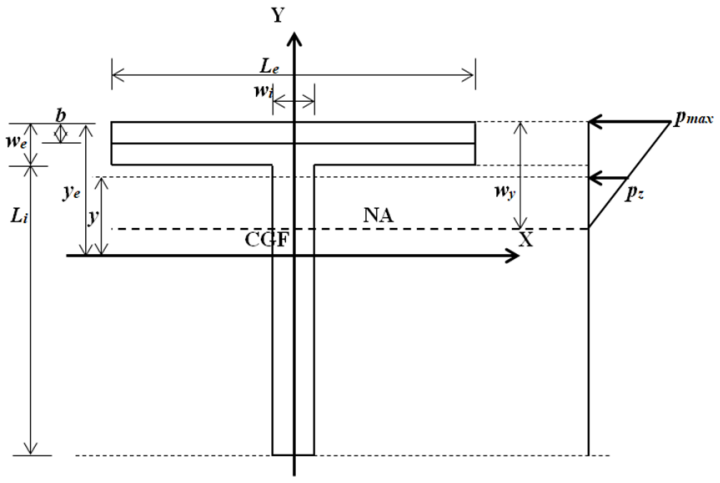

FIGURE 5. Case III

The resultant force is

$$R = -\int_{y_e - w_e}^{y_e} \int_{-\frac{L_e}{2}}^{\frac{L_e}{2}} p_z dx dy - n \int_{y_e - w_y}^{y_e - w_e} \int_{-\frac{w_i}{2}}^{\frac{w_i}{2}} p_z dx dy \tag{16}$$

Substituting Equation (11) into Equation (16) gives the following:

$$R = -\frac{p_{\max}\left[L_e w_e (2w_y - w_e) + n w_i (w_e - w_y)^2\right]}{2w_y} \tag{17}$$

The moment about the X axis is

$$M_x = -\int_{y_e-w_e}^{y_e}\int_{-\frac{L_e}{2}}^{\frac{L_e}{2}} p_z y dx dy - n\int_{y_e-w_y}^{y_e-w_e}\int_{-\frac{w_i}{2}}^{\frac{w_i}{2}} p_z y dx dy \tag{18}$$

Substituting Equation (11) into Equation (18) gives the following:

$$M_x = -\frac{p_{\max}\{w_e(L_e - nw_i)[2{w_e}^2 + 6w_y y_e - 3w_e(w_e + w_y)] + nw_i{w_y}^2(3y_e - w_y)\}}{6w_y} \tag{19}$$

2.4. **Optimal surface for strip footings.** The objective function to determine the minimum area "$A_{\min}$" for the three cases is

$$A_{\min} = L_e w_e + nL_i w_i \tag{20}$$

The constraint functions for the three cases are shown in Table 1.

TABLE 1. Constraint functions for strip footings

Case	Constraint functions
I	Equations (2) to (9), $P_1 = w_1 L_e$, $P_2 = nw_2(L_i + w_e - b)$, w_e and $w_i \geq b$, $w_i \leq L_e/n$, p_{s1} to $p_{s8} \leq p_{\max}$, $0 \leq p_{s1}$ to p_{s8}
II	Equations (13) and (15), $P_1 = w_1 L_e$, $P_2 = nw_2(L_i + w_e - b)$, w_e and $w_i \geq b$, $w_y \leq w_e$, $w_i \leq L_e/n$
III	Equations (17) and (19), $P_1 = w_1 L_e$ and $P_2 = nw_2(L_i + w_e - b)$, $w_e, w_i \geq b$, $w_y \geq w_e$, $w_i \leq L_e/n$

Figure 6 shows the flowchart to determine the minimum area of a strip footing to use Maple software.

This procedure is used as follows.

1) It starts with the parameters known as $p_{\max}$, w_1, w_2, L_e, b and n.

2) The objective function is determined by Equation (20).

3) The constraint functions for the three case are presented in Table 1.

4) Once the objective function and the constraint functions are known, the procedure presented in Figure 6 is used to determine the solution of the examples for Case I ($A_{\min}$, I_x, w_e, w_i, y_e, L_i, P_1, P_2, R, M_x, p_{s1}, p_{s3} and p_{s7}), and for Cases II and III ($A_{\min}$, w_e, w_i, L_i, P_1, P_2, R, M_x and w_y).

3. **Numerical Problems.** Eight examples for determining the minimum area "$A_{\min}$" and the dimensions of strip footings are shown in Tables 2 to 9. The general data for all examples are $L_e = 10.00$ m; $b = 0.30$ m. Example 1: The parameters are $w_e \neq w_i$, $w_1 = w_2 = 120$ kN/m, $p_{\max} = 200$ kN/m^2, $n = 1$, 2 and 3 (see Table 2). Example 2: The parameters are $w_e = w_i$, $w_1 = w_2 = 120$ kN/m, $p_{\max} = 200$ kN/m^2, $n = 1$, 2 and 3 (see Table 3). Example 3: The parameters are $w_e \neq w_i$, $w_1 = w_2 = 40$ kN/m, $p_{\max} = 200$ kN/m^2, $n = 1$, 2 and 3 (see Table 4). Example 4: The parameters are $w_e = w_i$, $w_1 = w_2 = 40$ kN/m, $p_{\max} = 200$ kN/m^2, $n = 1$, 2 and 3 (see Table 5). Example 5: The parameters are $w_e \neq w_i$, $w_1 = w_2 = 120$ kN/m, $p_{\max} = 300$ kN/m^2, $n = 1$, 2 and 3 (see Table 6). Example 6: The parameters are $w_e = w_i$, $w_1 = w_2 = 120$ kN/m, $p_{\max} = 300$ kN/m^2, $n = 1$, 2 and 3 (see Table 7). Example 7: The parameters are $w_e \neq w_i$, $w_1 = w_2 = 40$ kN/m, $p_{\max} = 300$ kN/m^2, $n = 1$, 2 and 3 (see Table 8). Example 8: The parameters are $w_e = w_i$, $w_1 = w_2 = 40$ kN/m, $p_{\max} = 300$ kN/m^2, $n = 1$, 2 and 3 (see Table 9). These examples are shown for walls located on property lines to demonstrate the advantages of this model.

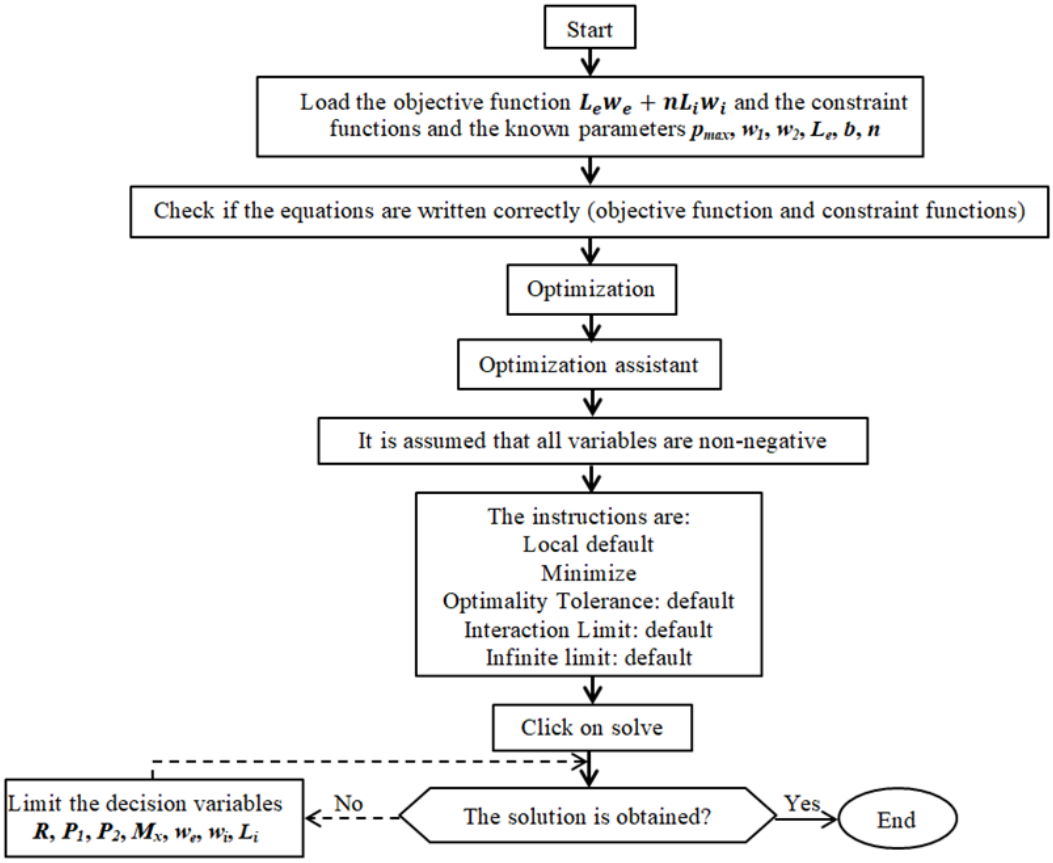

FIGURE 6. Flowchart for using Maple software

TABLE 2. Dimensions of the footings for $w_e \neq w_i$, $w_1 = w_2 = 120$ kN/m, $p_{\max} = 200$ kN/m^2

Case	n	P_1 (kN)	P_2 (kN)	R (kN)	M_x (kN-m)	L_i (m)	w_e (m)	w_i (m)	w_y (m)	p_{s1} (kN/m^2)	p_{s3} (kN/m^2)	p_{s7} (kN/m^2)	$p_{\max}$ (kN/m^2)	$A_{\min}$ (m^2)
I		1200.00	2583.39	3783.39	14460.70	21.51	0.32	1.48	–	200.00	197.06	0	200.00	35.14
II	1	1200.00	402.93	1602.93	2075.07	0	3.66	5.71	1.60	–	–	–	200.00	36.58
III		1200.00	607.02	1807.02	2849.00	4.57	0.79	3.65	2.61	–	–	–	200.00	24.59
I		1200.00	2509.57	3709.57	6650.37	0.06	10.70	5.00	–	68.97	0.39	0	68.97	107.57
II	2	1200.00	701.51	1901.51	1859.01	0	3.22	0.30	1.90	–	–	–	200.00	32.23
III		1200.00	1141.57	2341.57	3003.87	4.21	0.84	2.22	3.42	–	–	–	200.00	27.13
I		1200.00	2565.48	3765.48	4660.63	0	7.43	0.30	–	101.41	0	0	101.41	74.26
II	3	1200.00	1033.02	2233.02	1876.65	0.94	2.23	3.33	2.23	–	–	–	200.00	31.70
III		1200.00	1367.65	2567.65	2510.70	3.24	0.86	2.21	3.12	–	–	–	200.00	30.11

TABLE 3. Dimensions of the footings for $w_e = w_i$, $w_1 = w_2 = 120$ kN/m, $p_{\max} = 200$ kN/m^2

Case	n	P_1 (kN)	P_2 (kN)	R (kN)	M_x (kN-m)	L_i (m)	w_e (m)	w_i (m)	w_y (m)	p_{s1} (kN/m^2)	p_{s3} (kN/m^2)	p_{s7} (kN/m^2)	$p_{\max}$ (kN/m^2)	$A_{\min}$ (m^2)
I		1200.00	2454.40	3654.40	12640.15	10.75	10.00	10.00	–	35.22	18.25	0	35.22	207.53
II	1	1200.00	402.93	1602.93	2075.07	0	3.66	3.66	1.60	–	–	–	200.00	36.58
III		1200.00	1315.27	2515.27	7011.50	9.66	1.60	1.60	3.16	–	–	–	200.00	31.48
I		1200.00	2509.57	3709.57	6650.37	5.76	5.00	5.00	–	68.97	36.91	0	68.97	107.57
II	2	1200.00	701.51	1901.51	1859.01	0	3.22	3.22	1.90	–	–	–	200.00	32.23
III		1200.00	1751.82	2951.82	5199.77	6.24	1.36	1.36	4.64	–	–	–	200.00	30.58
I		1200.00	2565.48	3765.48	4660.63	4.09	3.33	3.33	–	101.41	55.89	0	101.41	74.26
II	3	1200.00	1033.02	2233.02	1876.65	0	3.17	3.17	2.23	–	–	–	200.00	31.70
III		1200.00	1227.77	2427.77	2233.95	1.28	2.43	2.43	2.43	–	–	–	200.00	33.62

TABLE 4. Dimensions of the footings for $w_e \neq w_i$, $w_1 = w_2 = 40$ kN/m, $p_{\max} = 200$ kN/m^2

Case	n	P_1 (kN)	P_2 (kN)	R (kN)	M_x (kN-m)	L_i (m)	w_e (m)	w_i (m)	w_y (m)	p_{s1} (kN/m^2)	p_{s3} (kN/m^2)	p_{s7} (kN/m^2)	$p_{\max}$ (kN/m^2)	$A_{\min}$ (m^2)
I		400.00	0	400.00	0	0	0.30	7.79	–	133.33	133.33	1333.33	133.33	3.00
II	1	400.00	17.72	417.72	29.08	0.33	0.42	0	0.42	–	–	–	200.00	4.18
III		400.00	22.20	422.20	17.98	0.55	0.30	0.30	0.50	–	–	–	200.00	3.17
I		400.00	0	400.00	0	0	0.30	0.30	–	133.33	133.33	1333.33	133.33	3.00
II	2	400.00	23.49	423.49	32.85	0.17	0.42	0.30	0.42	–	–	–	200.00	4.34
III		400.00	27.62	427.62	16.67	0.37	0.30	0.30	0.51	–	–	–	200.00	3.21
I		400.00	0	400.00	0	0	0.30	3.33	–	133.33	133.33	1333.33	133.33	3.00
II	3	400.00	26.69	426.69	32.55	0.10	0.43	0.30	0.43	–	–	–	200.00	4.35
III		400.00	30.30	430.30	15.56	0.25	0.30	0.30	0.51	–	–	–	200.00	3.23

TABLE 5. Dimensions of the footings for $w_e = w_i$, $w_1 = w_2 = 40$ kN/m, $p_{\max} = 200$ kN/m^2

Case	n	P_1 (kN)	P_2 (kN)	R (kN)	M_x (kN-m)	L_i (m)	w_e (m)	w_i (m)	w_y (m)	p_{s1} (kN/m^2)	p_{s3} (kN/m^2)	p_{s7} (kN/m^2)	$p_{\max}$ (kN/m^2)	$A_{\min}$ (m^2)
I		400.00	818.13	1218.13	4213.38	10.75	10.00	10.00	–	11.74	6.08	0	11.74	207.53
II	1	400.00	18.50	418.50	34.50	0.34	0.42	0.42	0.42	–	–	–	200.00	4.33
III		400.00	22.20	422.20	17.98	0.55	0.30	0.30	0.50	–	–	–	200.00	3.17
I		400.00	836.52	1236.52	2216.79	5.76	5.00	5.00	–	22.99	12.30	0	22.99	107.57
II	2	400.00	23.84	423.84	34.21	0.17	0.42	0.42	0.42	–	–	–	200.00	4.39
III		400.00	27.62	427.62	16.67	0.35	0.30	0.30	0.51	–	–	–	200.00	3.21
I		400.00	855.16	1255.16	1553.54	4.09	3.33	3.33	–	33.80	18.63	0	33.80	74.26
II	3	400.00	27.07	427.07	33.62	0.10	0.43	0.43	0.43	–	–	–	200.00	4.40
III		400.00	30.30	430.30	15.56	0.25	0.30	0.30	0.51	–	–	–	200.00	3.23

TABLE 6. Dimensions of the footings for $w_e \neq w_i$, $w_1 = w_2 = 120$ kN/m, $p_{\max} = 300$ kN/m^2

Case	n	P_1 (kN)	P_2 (kN)	R (kN)	M_x (kN-m)	L_i (m)	w_e (m)	w_i (m)	w_y (m)	p_{s1} (kN/m^2)	p_{s3} (kN/m^2)	p_{s7} (kN/m^2)	$p_{\max}$ (kN/m^2)	$A_{\min}$ (m^2)
I		1200.00	2454.40	3654.40	12640.15	9.31	11.44	10.00	–	35.22	15.80	0	35.22	207.53
II	1	1200.00	267.76	1467.76	1378.99	0	2.53	10.00	0.98	–	–	–	300.00	25.31
III		1200.00	655.58	1855.58	2939.10	5.25	0.52	1.69	2.73	–	–	–	300.00	14.01
I		1200.00	2771.76	2971.76	8269.12	11.55	0.30	0.91	–	300.00	292.40	0	300.00	24.09
II	2	1200.00	452.73	1652.73	1199.72	0.01	2.18	5.00	1.10	–	–	–	300.00	21.86
III		1200.00	886.11	2086.11	2223.88	3.45	0.54	1.56	2.34	–	–	–	300.00	16.20
I		1200.00	2565.48	3765.48	4660.63	0	7.43	3.32	–	101.41	0	0	101.41	74.26
II	3	1200.00	715.74	1915.74	1274.57	0.29	2.00	2.00	1.28	–	–	–	300.00	21.73
III		1200.00	643.60	1843.60	1169.20	0.86	1.23	3.33	1.23	–	–	–	300.00	20.88

TABLE 7. Dimensions of the footings for $w_e = w_i$, $w_1 = w_2 = 120$ kN/m, $p_{\max} = 300$ kN/m^2

Case	n	P_1 (kN)	P_2 (kN)	R (kN)	M_x (kN-m)	L_i (m)	w_e (m)	w_i (m)	w_y (m)	p_{s1} (kN/m^2)	p_{s3} (kN/m^2)	p_{s7} (kN/m^2)	$p_{\max}$ (kN/m^2)	$A_{\min}$ (m^2)
I		1200.00	2454.40	3654.40	12640.15	10.75	10.00	10.00	–	35.22	18.25	0	35.22	207.53
II	1	1200.00	267.76	1467.76	1378.99	0	2.53	2.53	0.98	–	–	–	300.00	25.31
III		1200.00	1210.01	2410.01	6252.36	9.11	1.27	1.27	1.70	–	–	–	300.00	24.33
I		1200.00	2509.57	3709.57	6650.37	5.76	5.00	5.00	–	68.97	36.91	0	68.97	107.57
II	2	1200.00	452.73	1652.73	1199.72	0	2.19	2.19	1.10	–	–	–	300.00	21.86
III		1200.00	1341.46	2541.46	3690.82	4.81	1.08	1.08	2.06	–	–	–	300.00	21.18
I		1200.00	2565.48	2765.48	4660.63	4.09	3.33	3.33	–	101.41	55.89	0	101.41	74.26
II	3	1200.00	643.60	1843.60	1169.20	0	2.09	2.09	1.23	–	–	–	300.00	20.88
III		1200.00	1112.90	2312.90	1993.93	1.85	1.54	1.54	1.54	–	–	–	300.00	23.97

TABLE 8. Dimensions of the footings for $w_e \neq w_i$, $w_1 = w_2 = 40$ kN/m, $p_{\max} = 300$ kN/m^2

Case	n	P_1 (kN)	P_2 (kN)	R (kN)	M_x (kN-m)	L_i (m)	w_e (m)	w_i (m)	w_y (m)	p_{s1} (kN/m^2)	p_{s3} (kN/m^2)	p_{s7} (kN/m^2)	$p_{\max}$ (kN/m^2)	$A_{\min}$ (m^2)
I		400.00	0	400.00	0	0	0.30	8.19	–	133.33	133.33	1333.33	133.33	3.00
II	1	400.00	37.40	437.40	23.09	0.94	0.30	0	0.29	–	–	–	300.00	3.00
III		400.00	50.00	450.00	95.62	1.25	0.30	0.64	0.30	–	–	–	300.00	3.80
I		400.00	0	400.00	0	0	0.30	0.30	–	133.33	133.33	1333.33	133.33	3.00
II	2	400.00	58.06	458.06	52.44	0.72	0.31	0.30	0.31	–	–	–	300.00	3.49
III		400.00	57.84	457.84	51.69	0.72	0.30	0.30	0.31	–	–	–	300.00	3.43
I		400.00	0	400.00	0	0	0.30	3.33	–	133.33	133.33	1333.33	133.33	3.00
II	3	400.00	70.29	470.29	53.96	0.57	0.31	0.30	0.31	–	–	–	300.00	3.65
III		400.00	69.52	462.52	52.08	0.58	0.30	0.30	0.31	–	–	–	300.00	3.52

TABLE 9. Dimensions of the footings for $w_e = w_i$, $w_1 = w_2 = 40$ kN/m, $p_{\max} = 300$ kN/m^2

Case	n	P_1 (kN)	P_2 (kN)	R (kN)	M_x (kN-m)	L_i (m)	w_e (m)	w_i (m)	w_y (m)	p_{s1} (kN/m^2)	p_{s3} (kN/m^2)	p_{s7} (kN/m^2)	$p_{\max}$ (kN/m^2)	$A_{\min}$ (m^2)
I		400.00	818.13	1218.13	7448.72	10.75	10.00	10.00	–	11.74	6.08	0	11.74	207.53
II	1	400.00	41.92	441.92	51.14	1.05	0.30	0.30	0.29	–	–	–	300.00	3.31
III		400.00	395.35	795.35	2025.00	9.81	0.38	0.38	0.63	–	–	–	300.00	7.45
I		400.00	836.52	1236.52	2216.79	5.76	5.00	5.00	–	22.99	12.30	0	22.99	107.57
II	2	400.00	58.27	458.27	53.10	0.72	0.31	0.31	0.31	–	–	–	300.00	3.50
III		400.00	57.84	457.84	51.69	0.72	0.30	0.30	0.31	–	–	–	300.00	3.43
I		400.00	855.16	1255.16	1553.54	4.09	3.33	3.33	–	33.80	18.63	0	33.80	74.26
II	3	400.00	71.10	471.10	55.75	0.58	0.31	0.31	0.31	–	–	–	300.00	3.69
III		400.00	69.52	469.52	52.08	0.58	0.30	0.30	0.31	–	–	–	300.00	3.52

4. **Results.** Table 2 shows the first example and the following can be observed: In all cases P_1 is constant. As n increases, P_2 and R tend to decrease until $n = 2$ and then increases in Case I and in Cases II and III it increases; M_x tends to decrease in Case I, in Case II it tends to decrease until $n = 2$ and then increases and in Case III it tends to increase until $n = 2$ and then decreases; L_i tends to decrease in Cases I and III, in Case II it is zero for $n = 1$ and 2 and in $n = 3$ it has value; w_e and $A_{\min}$ tend to increase until $n = 2$ and then decrease in Case I, in Case II it tends to decrease and in Case III it tends to increase; w_i tends to increase until $n = 2$ and then decrease in Case I, in Case II it tends to decrease until $n = 2$ and then increase and in Case III it tends to decrease. The smallest $A_{\min}$ for each n appears in Case III and the largest $A_{\min}$ for each n appears in Case I.

Table 3 presents the second example and the following can be observed: In all cases P_1 is constant. As n increases, P_2 and R tend to increase in Cases I and II and in Case III tends to increase until $n = 2$ and then decreases; M_x tends to decrease in Cases I and III, it tends to decrease until $n = 2$ and then increases; L_i tends to decrease in Cases I and III, in Case II it is zero for all cases; w_e, w_i and $A_{\min}$ tend to decrease in Cases I and II and in Case III it tends to decrease until $n = 2$ and then increase. The smallest $A_{\min}$ for each n appears in Case III for $n = 1$ and 2 and in Case II for $n = 3$ and the largest $A_{\min}$ for each n appears in Case I.

Table 4 shows the third example and the following can be observed: In all cases P_1 is constant. As n increases, P_2 and R are constant in Case I and in Cases II and III they tend to increase; M_x is zero in Case I, in Case II it tends to increase until $n = 2$ and then decreases and in Case III it tends to decrease; L_i is zero in Case I, in Cases II and III it tends to decrease; w_e is constant in Cases I and III and in Case II it is constant in n

= 1 and 2 and in $n = 3$ it increases; w_i tends to decrease until $n = 2$ and then increase in Case I, in Case II it tends to increase until $n = 2$ and then it is constant and in Case III it is constant; $A_{\min}$ is constant in Case I and in Cases II and III it tends to increase; The smallest $A_{\min}$ for each n appears in Case I and the largest $A_{\min}$ for each n appears in Case II.

Table 5 presents the fourth example and the following can be observed: In all cases P_1 is constant. As n increases, P_2 and R tend to increase in all cases; M_x and L_i tend to decrease in all cases; w_e and w_i tend to decrease in Case I, in Case II it is constant in $n =$ 1 and 2 and in $n = 3$ it increases and in Case III it is constant; $A_{\min}$ tends to decrease in Cases I and III and in Case II it tends to increase. The smallest $A_{\min}$ for each n appears in Case III and the largest $A_{\min}$ for each n appears in Case I.

Table 6 shows the fifth example and the following can be observed: In all cases P_1 is constant. As n increases, P_2 and R tend to increase until $n = 2$ and then decrease in Cases I and III and in Case II it increases; M_x tends to decrease in Case I, in Case II it tends to decrease until $n = 2$ and then increases and in Case III it tends to decrease; L_i tends to increase until $n = 2$ and at $n = 3$ it is zero, in Case II it tends to increase and in Case III it tends to decrease; w_e and $A_{\min}$ tend to decrease until $n = 2$ and then increase in Case I, in Case II it tends to decrease and in Case III it tends to increase; w_i tends to decrease until $n = 2$ and then increase in Cases I and III and in Case II it tends to decrease. The smallest $A_{\min}$ for each n appears in Case III and the largest $A_{\min}$ for each n appears in Case I.

Table 7 presents the sixth example and the following can be observed: In all cases P_1 is constant. As n increases, P_2 and R tend to increase in Cases I and II and in Case III tends to increase until $n = 2$ and then decreases; M_x tends to decrease in Cases I, II and III; L_i tends to decrease in Cases I and III, in Case II it is zero for all cases; w_e, w_i and $A_{\min}$ tend to decrease in Cases I and II and in Case III it tends to decrease until $n = 2$ and then increase. The smallest $A_{\min}$ for each n appears in Case III for $n = 1$ and 2 and in Case II for $n = 3$ and the largest $A_{\min}$ for each n appears in Case I.

Table 8 shows the seventh example and the following can be observed: In all cases P_1 is constant. As n increases, P_2 and R are constant in Case I and in Cases II and III they tend to increase; M_x is zero in Case I, in Case II it tends to increase and in Case III it tends to decrease until $n = 2$ and then increase; L_i is zero in Case I and in Cases II and III it tends to decrease; w_e is constant in Cases I and III and in Case II it is constant in n = 1 and in $n = 2$ and 3 it increases; w_i tends to decrease until $n = 2$ and then increases in Case I, in Case II is zero in $n = 1$ and in $n = 2$ and 3 it increases and in Case III it tends to decrease; $A_{\min}$ is equal in Case I, in Case II it tends to increase and in Case III it tends to decrease. The smallest $A_{\min}$ for each n appears in Case I and the largest $A_{\min}$ for each n appears in Case III for $n = 1$ and in Case II for $n = 2$ and 3.

Table 9 presents the eighth example and the following can be observed: In all cases P_1 is constant. As n increases, P_2 and R tend to increase in Cases I and II and in Case III tend to increase until $n = 2$ and then increase; M_x tends to decrease in Case I, in Case II it tends to increase and in Case III it tends to decrease until $n = 2$ and then increases; L_i tends to decrease in all cases; w_e and w_i tend to decrease in Cases I and III and in Case II it tends to increase; $A_{\min}$ tends to decrease in Case I, in Case II it tends to increase and in Case III it tends to decrease until $n = 2$ and then increase. The smallest $A_{\min}$ for each n appears in Case II for $n = 1$ and in Case III for $n = 2$ and 3 and the largest $A_{\min}$ for each n appears in Case I.

Figure 7 shows the minimum areas for the strip footings of the eight examples.

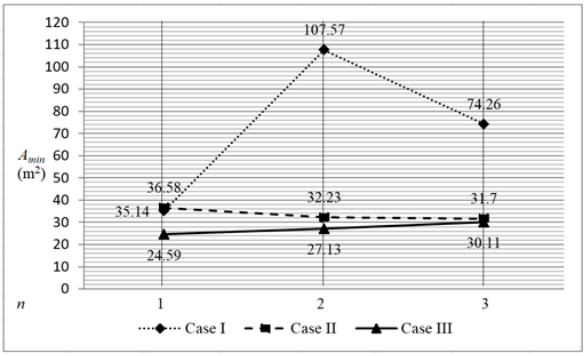

(a) Example 1

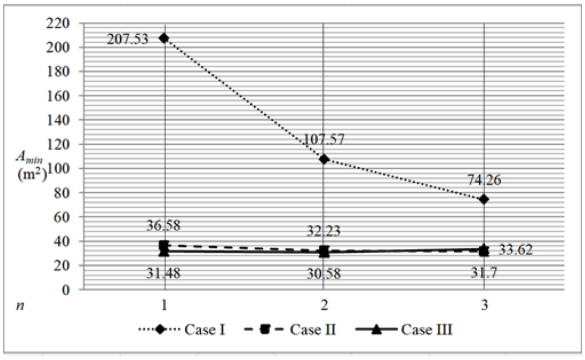

(b) Example 2

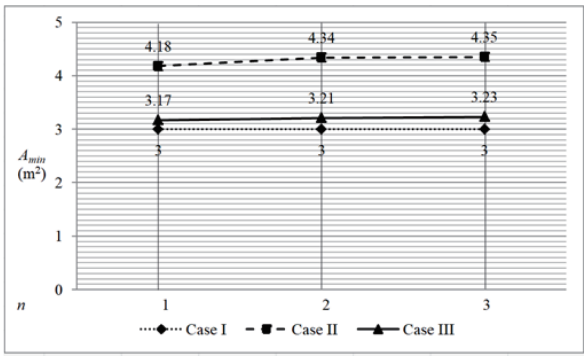

(c) Example 3

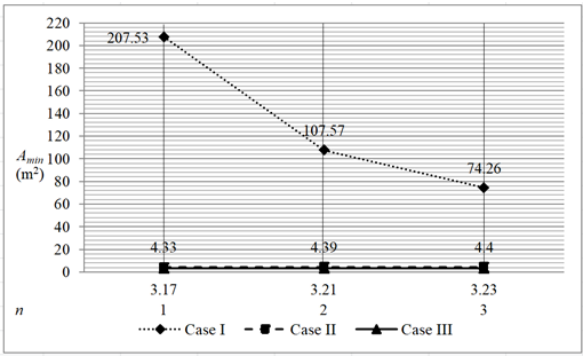

(d) Example 4

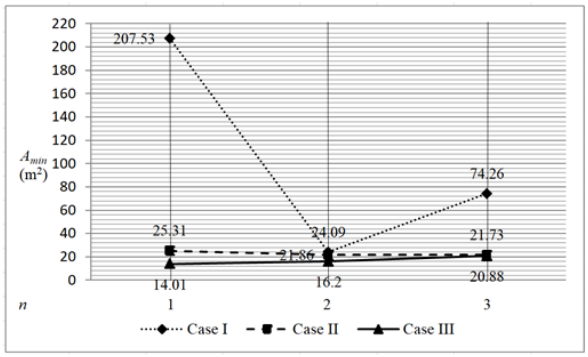

(e) Example 5

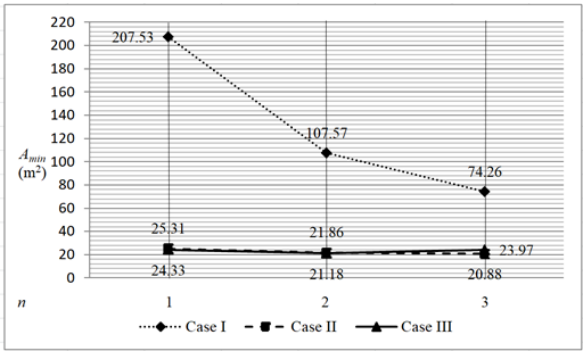

(f) Example 6

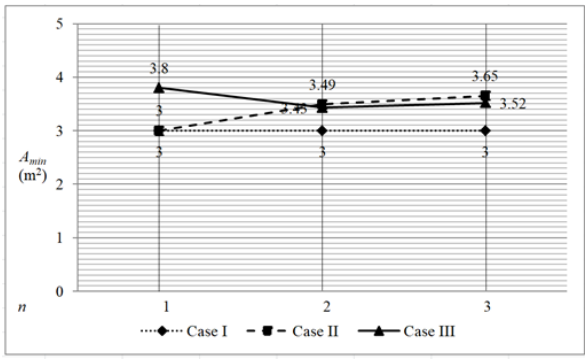

(g) Example 7

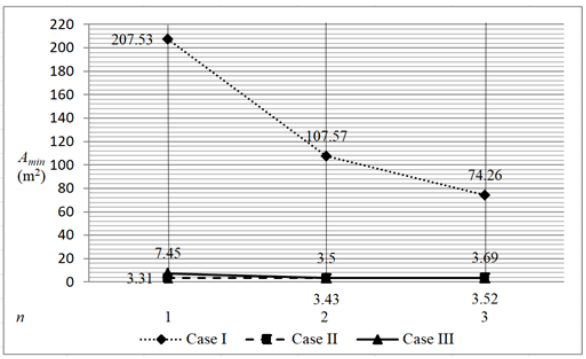

(h) Example 8

FIGURE 7. Minimum areas for strip footings of the eight examples

Figure 7(a) presents a difference of 1.04 (Case II) and 0.70 (Case III) in $n = 1$, in $n = 2$ they have a difference of 0.30 (Case II) and 0.25 (Case III), and $n = 3$ they have a difference of 0.43 (Case II) and 0.41 (Case III) with respect to Case I.

Figure 7(b) shows a difference of 0.18 (Case II) and 0.15 (Case III) in $n = 1$, in $n = 2$ they have a difference of 0.30 (Case II) and 0.28 (Case III), and $n = 3$ they have a difference of 0.43 (Case II) and 0.45 (Case III) with respect to Case I.

Figure 7(c) presents a difference of 1.39 (Case II) and 1.06 (Case III) in $n = 1$, in $n = 2$ they have a difference of 1.45 (Case II) and 1.07 (Case III), and $n = 3$ they have a difference of 1.45 (Case II) and 1.08 (Case III) with respect to Case I.

Figure 7(d) shows a difference of 0.02 (Case II) and 0.02 (Case III) in $n = 1$, in $n = 2$ they have a difference of 0.04 (Case II) and 0.03 (Case III), and $n = 3$ they have a difference of 0.06 (Case II) and 0.04 (Case III) with respect to Case I.

Figure 7(e) presents a difference of 0.12 (Case II) and 0.07 (Case III) in $n = 1$, in $n = 2$ they have a difference of 0.91 (Case II) and 0.67 (Case III), and $n = 3$ they have a difference of 0.29 (Case II) and 0.28 (Case III) with respect to Case I.

Figure 7(f) shows a difference of 0.12 (Case II) and 0.12 (Case III) in $n = 1$, in $n = 2$ they have a difference of 0.20 (Case II) and 0.20 (Case III), and $n = 3$ they have a difference of 0.28 (Case II) and 0.32 (Case III) with respect to Case I.

Figure 7(g) presents a difference of 1.00 (Case II) and 1.27 (Case III) in $n = 1$, in $n = 2$ they have a difference of 1.16 (Case II) and 1.15 (Case III), and $n = 3$ they have a difference of 1.22 (Case II) and 1.17 (Case III) with respect to Case I.

Figure 7(h) shows a difference of 0.02 (Case II) and 0.04 (Case III) in $n = 1$, in $n = 2$ they have a difference of 0.03 (Case II) and 0.03 (Case III), and $n = 3$ they have a difference of 0.05 (Case II) and 0.05 (Case III) with respect to Case I.

5. **Conclusions.**

This paper presents a model to estimate the minimum surface in plan of a strip footing supporting a masonry wall or a concrete wall (uniformly distributed load), assuming that the soil is elastic, the soil pressure distribution is linear and the surface in contact with the soil works partiality in compression.

In this investigation three cases are shown. Case I: When the area works totally in compression or current model. Case II: When the area works partially in compression and the neutral axis falls within the flanges. Case III: When the area works partially in compression and the neutral axis falls within the web.

This work consists of estimating the width (w_e and w_i), inner wall length (L_i) and the position where pressure is zero "w_y" of a strip footing subjected to uniaxial bending, taking account of the objective function (minimum area) and the constraint functions that shows in Table 1.

The contributions of this paper are as follows.

1) Some works assume uniform soil pressure with the wall located at the center of the footing, but do not consider the property boundaries that may occur in some cases.

2) The minimum area in Case I appears when the soil pressure on the footing is uniform for all n (see Tables 4 and 8).

3) When w_i or L_i are equal to zero, the footing is rectangular (see Tables 2, 3, 4, 6, 7 and 8).

4) When P_2 and M_x are equal to zero, the footing is rectangular (see Tables 4 and 8). This means that the resultant force is located in the center of the footing.

5) The minimum area in Case II appears in $n = 3$, when $w_e = w_i$ and $w_e \geq w_y$ (see Tables 3 and 7).

6) The main savings with respect to Case I occur at $n = 1$ for $w_e \neq w_i$ with 93.25%, while for $w_e = w_i$ with 98.47%.

7) This model can be applied to different soil types, structural loads or geographical regions [16].

Future suggestions for the research are

1) Experimental analysis of the plan surface for strip footings assuming that the contact surface with the ground works partially under compression;

2) Minimum cost design for a strip footing taking account of that the area in contact with the soil works partially in compression;

3) Minimum area in plan for a strip footing supporting an entire building, assuming that the surface in contact with the ground works partially under compression.

REFERENCES

[1] J. Khazaie and S. A. Amirshahkarami, Numerical analysis of interaction between earth and large foundations regarding size effect, *Journal of Applied Sciences*, vol.9, no.6, pp.1036-1045, 2009.

[2] M. Jahanandish, M. Veiskarami and A. Ghahramani, Effect of foundation size and roughness on the bearing capacity factor, N_γ, by stress level-based ZEL method, *Arabian Journal for Science and Engineering*, vol.37, no.7, pp.1817-1831, 2012.

[3] G. A. Vyacheslavovich and B. L. Adolfovich, Influence of the form and size of the isolated foundations on the stress-strain state of the soil base, *Journal of Applied Engineering Science*, vol.14, no.1, pp.28-35, 2016.

[4] S. López-Chavarría, A. Luévanos-Rojas and M. Medina-Elizondo, A mathematical model for dimensioning of square isolated footings using optimization techniques: General case, *International Journal of Innovative Computing, Information and Control*, vol.13, no.1, pp.67-74, 2017.

[5] S. López-Chavarría, A. Luévanos-Rojas and M. Medina-Elizondo, Optimal dimensioning for the corner combined footings, *Advances in Computational Design*, vol.2, no.2, pp.169-183, 2017.

[6] A. Luévanos-Rojas, A mathematical model for dimensioning of footings square, *International Review of Civil Engineering*, vol.3, no.4, pp.346-350, 2012.

[7] A. Luévanos-Rojas, A mathematical model for the dimensioning of circular footings, *Far East Journal of Mathematical Sciences*, vol.71, no.2, pp.357-367, 2012.

[8] A. Luévanos-Rojas, A mathematical model for dimensioning of footings rectangular, *ICIC Express Letters, Part B: Applications*, vol.4, no.2, pp.269-274, 2013.

[9] W. L. Filho, R. C. H. Carvalho, A. L. Christoforo and F. A. R. Lahr, Dimensioning of isolated footing submitted to the under biaxial bending considering the low concrete consumption, *International Journal of Materials Engineering*, vol.7, no.1, pp.1-11, 2017.

[10] A. Luévanos-Rojas, A comparative study for dimensioning of footings with respect to the contact surface on soil, *International Journal of Innovative Computing, Information and Control*, vol.10, no.4, pp.1313-1326, 2014.

[11] A. Luévanos-Rojas, A new mathematical model for dimensioning of the boundary trapezoidal combined footings, *International Journal of Innovative Computing, Information and Control*, vol.11, no.4, pp.1269-1279, 2015.

[12] A. Luévanos-Rojas, A mathematical model for the dimensioning of combined footings of rectangular shape, *Revista Técnica de la Facultad de Ingeniería Universidad del Zulia*, vol.39, no.1, pp.3-9, 2016.

[13] A. Luévanos-Rojas, S. López-Chavarría and M. Medina-Elizondo, A new model for T-shaped combined footings Part I: Optimal dimensioning, *Geomechanics and Engineering*, vol.14, no.1, pp.51-60, 2018.

[14] G. Aguilera-Mancilla, A. Luévanos-Rojas, S. López-Chavarría and M. Medina-Elizondo, Modeling for the strap combined footings Part I: Optimal dimensioning, *Steel and Composite Structures*, vol.30, no.2, pp.97-108, 2019.

[15] M. A. Moreno-Hernandez, A. Luévanos-Rojas, S. López-Chavarría and M. Medina-Elizondo, Mathematical modeling for corner strap combined footings resting on the ground: Part 1, *Computación y Sistemas*, vol.26, no.3, pp.1259-1272, 2022.

[16] M. I. L. Ávila-García, A. Luévanos-Rojas, C. Martinez-Aguilar and L. L. Gaona-Tamez, Optimal area for rectangular foundation slabs in plan supported on soil, *International Journal of Innovative Computing, Information and Control*, vol.20, no.5, pp.1399-1413, 2024.

[17] A. Luévanos-Rojas, J. G. Faudoa-Herrera, R. A. Andrade-Vallejo and M. A. Cano-Alvarez, Design of isolated footings of rectangular form using a new model, *International Journal of Innovative Computing, Information and Control*, vol.9, no.10, pp.4001-4022, 2013.

[18] S. López-Chavarría, A. Luévanos-Rojas and M. Medina-Elizondo, A new mathematical model for design of square isolated footings for general case, *International Journal of Innovative Computing, Information and Control*, vol.13, no.4, pp.1149-1168, 2017.
[19] A. Luévanos-Rojas, Design of isolated footings of circular form using a new model, *Structural Engineering and Mechanics*, vol.52, no.4, pp.767-786, 2014.
[20] A. Luévanos-Rojas, Minimum cost design for rectangular isolated footings taking into account that the column is located in any part of the footing, *Buildings*, vol.13, no.9, pp.1-16, 2023.
[21] A. Luévanos-Rojas, V. M. Moreno-Landeros, G. Santiago-Hurtado, F. J. Olguin-Coca, L. D. López-León and E. R. Diaz-Gurrola, Mathematical modeling for the optimal cost design of circular isolated footings with eccentric column, *Mathematics*, vol.12, no.5, pp.1-19, 2024.
[22] A. Luévanos-Rojas, Design of boundary combined footings of rectangular shape using a new model, *DYNA Colombia*, vol.81, no.188, pp.199-208, 2014.
[23] A. Luévanos-Rojas, A new model for the design of rectangular combined boundary footings with two restricted opposite sides, *Revista ALCONPAT*, vol.6, no.2, pp.172-187, 2016.
[24] A. Luévanos-Rojas, S. López-Chavarría and M. Medina-Elizondo, A new model for T-shaped combined footings Part II: Mathematical model for design, *Geomechanics and Engineering*, vol.14, no.1, pp.61-69, 2018.
[25] J. A. Yáñez-Palafox, A. Luévanos-Rojas, S. López-Chavarría and M. Medina-Elizondo, Modeling for the strap combined footings Part II: Mathematical model for design, *Steel and Composite Structures*, vol.30, no.2, pp.109-121, 2019.
[26] A. Luévanos-Rojas, S. López-Chavarría, M. Medina-Elizondo, R. Sandoval-Rivas and O. M. Farías-Montemayor, An analytical model for the design of corner combined footings, *Revista ALCONPAT*, vol.10, no.3, pp.317-335, 2020.
[27] M. L. Garcia-Graciano, A. Luévanos-Rojas, S. López-Chavarría and M. Medina-Elizondo, Mathematical modeling for corner strap combined footings resting on the ground: Part 2, *Computación y Sistemas*, vol.26, no.4, pp.1429-1443, 2022.
[28] A. Luévanos-Rojas, Optimization for trapezoidal combined footings: Optimal design, *Advances in Concrete Construction*, vol.16, no.1, pp.21-34, 2023.
[29] A. Luévanos-Rojas, G. Santiago-Hurtado, V. M. Moreno-Landeros, F. J. Olguin-Coca, L. D. López-León and E. R. Diaz-Gurrola, Mathematical modeling of the optimal cost for the design of strap combined footings, *Mathematics*, vol.12, no.2, pp.1-20, 2024.
[30] R. Irles-Más and F. Irles-Más, Explicit stresses under rectangular detached footings with biaxial bending, *Informes de la Construcción*, vol.44, no.419, pp.77-90, 1992.
[31] H. M. Algin, Stresses from linearly distributed pressures over rectangular areas, *International Journal Numerical Analytical Methods in Geomechanics*, vol.24, no.8, pp.681-692, 2000.
[32] H. M. Algin, Practical formula for dimensioning a rectangular footing, *Engineering Structures*, vol.29, no.6, pp.1128-1134, 2007.
[33] G. Özmen, Determination of base stresses in rectangular footings under biaxial bending, *Teknik Dergi Digest*, vol.22, no.4, pp.1519-1535, 2011.
[34] J. Bellos and N. P. Bakas, High computational efficiency through generic analytical formulation for linear soil pressure distribution of rigid spread rectangular footings, *Proc. of the 7th European Congress on Computational Methods in Applied Sciences and Engineering*, Crete Island, Greece, 2016.
[35] J. Bellos and N. P. Bakas, Complete analytical solution for linear soil pressure distribution under rigid rectangular spread footings, *International Journal of Geomechanics*, vol.17, no.7, DOI: 10.1061/(ASCE)GM.1943-5622.0000874, 2017.
[36] I. Aydogdu, New iterative method to calculate base stress of footings under biaxial bending, *International Journal of Engineering & Applied Sciences (IJEAS)*, vol.8, no.4, pp.40-48, 2016.
[37] K. Girgin, Simplified formulations for the determination of rotational spring constants in rigid spread footings resting on tensionless soil, *Journal of Civil Engineering and Management*, vol.23, no.4, pp.464-474, 2017.
[38] V. B. Vela-Moreno, A. Luévanos-Rojas, S. López-Chavarría, M. Medina-Elizondo, R. Sandoval-Rivas and C. Martínez-Aguilar, Optimal area for rectangular isolated footings considering that contact surface works partially to compression, *Structural Engineering and Mechanics*, vol.84, no.4, pp.561-573, 2022.
[39] V. M. Moreno-Landeros, A. Luévanos-Rojas, G. Santiago-Hurtado, L. D. López-León and E. R. Diaz-Gurrola, Optimal area for a rectangular isolated footing with an eccentric column and partial ground compression, *Applied Sciences*, vol.14, no.15, pp.1-16, 2024.

[40] S. Soto-Garcia, A. Luévanos-Rojas, J. D. Barquero-Cabrero, S. López-Chavarría, M. Medina-Elizondo, O. M. Farias-Montemayor and C. Martínez-Aguilar, A new model for the contact surface with soil of circular isolated footings considering that the contact surface works partially under compression, *International Journal of Innovative Computing, Information and Control*, vol.18, no.4, pp.1103-1116, 2022.

[41] I. Luévanos-Soto, A. Luévanos-Rojas, V. M. Moreno-Landeros and G. Santiago-Hurtado, Minimum area for circular isolated footings with eccentric column taking into account that the surface in contact with the ground works partially in compression, *Coupled Systems Mechanics*, vol.13, no.3, pp.201-217, 2024.

[42] A. Luévanos-Rojas, B. L. Estrada-Mendoza and M. Juárez-Ramirez, Comparative study for minimum areas in contact with the ground of rectangular and circular isolated footings working partially under compression, *Boletín Ciencias de la Tierra*, vol.55, no.1, pp.85-98, 2024.

[43] P. Montes-Paramo, A. Luévanos-Rojas, S. López-Chavarría, M. Medina-Elizondo and R. Sandoval-Rivas, Optimal area for rectangular combined footings assuming that contact surface with the soil works partially to compression, *Ingeniería Investigación y Tecnología*, vol.24, no.2, pp.1-15, 2023.

[44] A. Luévanos-Rojas, New model for complete design of rectangular isolated footings taking into account that the contact surface works partially in compression, *Revista ALCONPAT*, vol.13, no.2, pp.192-219, 2023.

[45] D. S. Kim-Sánchez, A. Luévanos-Rojas, J. D. Barquero-Cabrero, S. López-Chavarría, M. Medina-Elizondo and I. Luévanos-Soto, A new model for the complete design of circular isolated footings considering that the contact surface works partially under compression, *International Journal of Innovative Computing, Information and Control*, vol.18, no.6, pp.1769-1784, 2022.

[46] I. Luévanos-Soto, A. Luévanos-Rojas, V. M. Moreno-Landeros and G. Santiago-Hurtado, Minimum cost design for circular isolated footings with eccentric column taking into account that the surface in contact with the ground works partially in compression, *Coupled Systems Mechanics*, vol.13, no.4, pp.311-335, 2024.

[47] N. M. Saleh, A. E. Alsaied and A. M. Elleboudy, Performance of skirted strip footing subjected to eccentric inclined load, *Electronic Journal of Geotechnical Engineering*, vol.13, no.1, pp.1-13, 2008.

[48] N. M. Saleh, A. M. Elleboudy and A. E. Elsaied, Behavior of skirted strip footing under eccentric load, *Proc. of the 17th International Conference on Soil Mechanics and Geotechnical Engineering*, Alexandria, Egypt, 2009.

[49] O. Farzaneh, J. Mofidi and F. Askari, Seismic bearing capacity of strip footings near cohesive slopes using lower bound limit analysis, *Proc. of the 18th International Conference on Soil Mechanics and Geotechnical Engineering*, Paris, France, 2013.

[50] E. Sadoglu, Design optimization for symmetrical gravity retaining walls, *Acta Geotechnica Slovenica*, vol.11, no.2, pp.70-79, 2014.

[51] W. Fang and L.-J. Shi, Lower bound solution of foundation bearing capacity beneath strip footing based on parabolic Mohr failure criterion, *Advances in Civil Engineering*, vol.2020, pp.1-8, DOI: 10.1155/2020/8897777, 2020.

[52] S. Keawsawasvong and B. Ukritchon, A practical method for the optimal design of continuous footing using ant-colony optimization, *Acta Geotechnica Slovenica*, vol.12, no.2, pp.45-55, 2016.

[53] B. Mazouz, T. Mansouri, M. Baazouzi and K. Abbeche, Assessing the effect of underground void on strip footing sitting on a reinforced sand slope with numerical modeling, *Engineering, Technology & Applied Science Research*, vol.12, no.4, pp.9005-9011, 2022.

[54] N. Yalaoui, H. Trouzine, M. Meghachou and T. Miranda, Geotextile reinforced strip footing: Numerical modeling and analysis, *Mathematical Modelling of Engineering Problems*, vol.10, no.2, pp.398-404, 2023.

[55] S. S. Pusadkar, S. S. Harne and S. W. Thakare, Performance of strip footing above multiple square voids in C-$\emptyset$ soil, *International Journal of Engineering Research & Technology (IJERT)*, vol.6, no.6, pp.816-823, 2017.

[56] S. Jaiswal, A. Srivastava and V. B. Chauhan, Performance of strip footing on sand bed reinforced with multilayer geotextile with wraparound ends, *Proc. of Indian Geotechnical Conference 2020*, Andhra University, Visakhapatnam, Indian, 2020.

Author Biography

Inocencio Luévanos-Soto graduated as an Architect (2009), Master in Science with Specialization in Planning and Construction of Works (2012), and Doctor in Engineering with Specialization in Planning Systems and Construction (2024), all these from the Facultad de Ingeniería, Arquitectura, Gómez Palacio Campus of the Universidad Juárez del Estado de Durango. He is professor and researcher of the Facultad de Ingeniería, Ciencias y Arquitectura, Gómez Palacio Campus of the Universidad Juárez del Estado de Durango from since 2010 to date. His research interests are mathematical models applied to Engineering and Architect.

Arnulfo Luévanos-Rojas received his B.Sc. degree in Civil Engineering (1981), from the Facultad de Ingeniería, Arquitectura, Gómez Palacio Campus of the Universidad Juárez del Estado de Durango. Master in Science with Specialization in Structures (1983), from the Facultad de Ingeniería y Arquitectura, Distrito Federal Campus of the Instituto Politécnico Nacional. Master in Science with Specialization in Planning and Construction of Works (2000), from the Facultad de Ingeniería, Arquitectura, Gómez Palacio Campus of the Universidad Juárez del Estado de Durango. Master in Administration (2004), from the Facultad de Contaduría y Administración, Torreón Campus of the Universidad Autónoma de Coahuila. And Doctor in Engineering with Specialization in Planning Systems and Construction (2009), from the Facultad de Ingeniería, Arquitectura, Gómez Palacio Campus of the Universidad Juárez del Estado de Durango. He was professor and researcher of the Facultad de Ingeniería, Ciencias y Arquitectura, Gómez Palacio Campus of the Universidad Juárez del Estado de Durango from 2006 to 2015, and of the Facultad de Contaduría y Administración, Torreón campus of the Universidad Autónoma de Coahuila since 2015 to date. He has published more than 139 papers in journals indexed in the Web of Science. His research interests are mathematical models applied to Engineering and Administration. He is member of the National System of Researchers of Mexico (Level I from 2016-2022 and Level II from 2023-2027). He is an Honorary State Researcher for the State of Coahuila, Mexico. He has received several distinctions: Distinguished Professor by ULSA (Universidad La Salle Laguna) 2002, 2007, 2010; Researcher of the year 2023 by UAC (Universidad Autónoma de Coahuila); Best scientific article of the year 2023 by UAC (Universidad Autónoma de Coahuila); He has been included in the "2023 World's Top 2% Scientists List" by Stanford University.

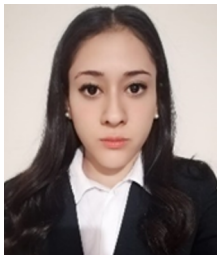

Rosa Margarita Luévanos-Soto received the Master's degree in Administration and Senior Management (2020) and the degree of Doctor in Administration and Senior Management (2024) from the Facultad de Contaduría y Administración of the Universidad Autónoma de Coahuila. She is professor and researcher of the Facultad de Contaduría y Administración, Torreón campus of the Universidad Autónoma de Coahuila. Her research interests are mathematical models applied to Administration.